Journal of Physics and Chemistry of Solids 171 (2022) 111001

Contents lists available at ScienceDirect

Journal of Physics and Chemistry of Solids

journal homepage: www.elsevier.com/locate/jpcs

Role of Fe atom valence states and oxygen vacancies in substituted lanthanum ferrite $La_{0.67}Sr_{0.33}FeO_{3-\gamma}$

V. Sedykh [a,**], O. Rybchenko [a], V. Rusakov [b], S. Zaitsev [a], O. Barkalov [a], E. Postnova [a], T. Gubaidulina [b], D. Pchelina [b,*], V. Kulakov [a]

[a] Institute of Solid State Physics, Russian Academy of Sciences, Chernogolovka, 142432, Russia
[b] Lomonosov Moscow State University, Moscow, 119991, Russia

ARTICLE INFO

Keywords:
Perovskites
Substituted lanthanum ferrites
Mössbauer spectroscopy
X-ray diffraction
Raman spectroscopy
Fe valence states
Oxygen vacancies

ABSTRACT

The substituted orthoferrite $La_{0.67}Sr_{0.33}FeO_{3-\gamma}$ was studied using scanning electron microscopy, X-ray diffraction (XRD), and Mössbauer and Raman spectroscopy. A series of vacuum annealing in the temperature range of 200–650 °C was performed, resulting in negligible changes in the crystal structure of samples. The volume of the pseudocubic unit cell increased continuously with raising temperature up to 450 °C. It follows from the Mössbauer measurements that at room temperature Fe ions were characterized by an averaged-valence state. The vacuum annealing induced oxygen vacancies and changed the averaged-valence state of Fe ions. Sufficiently good correlations among the Mössbauer, XRD, and Raman spectroscopy data were obtained.

1. Introduction

Perovskite-type oxides $R_{1-x}A_xBO_{3-\gamma}$ (R = rare-earth element; A = Ba, Ca, or Sr; and B = Fe, Mn, Co or Ni) are promising materials due to their unusual electrical, magnetic, and catalytic properties [1,2]. In these systems, transition metal ions have mixed valence states, which are responsible for high electronic conductivity near room temperature. These states can lead to significant oxygen nonstoichiometry, which is the result of a high level of oxygen ion diffusion. Mixed valence can be caused either by the substitution of divalent ions (A) for the trivalent element (R) positions, or by the formation of oxygen vacancies [3]. Magnetic properties of these complexes are assumed to be the result of a superexchange mechanism involving 3 *d* electrons of transition metal ions and the *p* orbital of oxygen [4]. Thus, oxygen plays a very important role in the magnetic order of these compounds.

Materials belonging to this family with the composition RBO_3 have perovskite-like crystal structures. Compounds with the Fe metal ion (B) are called orthoferrites, and have a distorted perovskite structure. Distortions are associated with the displacement of oxygen and rare-earth ions from the positions corresponding to the cubic structure [5,6].

Orthoferrite $LaFeO_3$ is multiferroic and, thus, is one of the most important members of the RBO_3 family [7]. Various applications are possible, including as electrode materials for fuel elements, catalysts, chemical sensors, optoelectronic devices, and magnetic memory devices [8–12]. It has an orthorhombic structure with the space group *Pbnm*; the Fe ions are in a trivalent state and have an octahedral oxygen environment. Oxygen anions located at the vertices of the octahedron participate in the superexchange interaction between Fe ions Fe^{3+}–O^{2-}–Fe^{3+}. According to the Goodenough theory [13], the superexchange interaction between $3d^5$ (Fe^{3+}) and $3d^5$ (Fe^{3+}) cations is antiferromagnetic and stronger than between Fe^{4+} and Fe^{3+}, as well as among Fe^{4+} ions. Oxygen octahedra are arranged in a zigzag manner along the *c* axis of a crystalline lattice; as a result the linkage angle Fe^{3+}–O^{2-}–Fe^{3+} deviates from 180°. The increase of the superexchange interaction between Fe^{3+} ions with the Fe^{3+}–O^{2-}–Fe^{3+} linkage angle [6] was reported for $LaFeO_3$ orthoferrite [7,13].

When trivalent La^{3+} is partially replaced by divalent Sr^{2+}, a homogeneous structural and charge ordering in $La_{1-x}Sr_xFeO_{3-\gamma}$ oxides is violated on a local level. There is some uncertainty in determining their structures for $x < 0.4$ compositions. The rhombohedral, orthorhombic crystalline lattices or their mixture have been proposed [14,15]. The oxidation state of Fe ions increases from Fe^{3+} to Fe^{4+} when La^{3+} cations are substituted by Sr^{2+} in $LaFeO_{3-\gamma}$. This weakens the antiferromagnetic order caused by the superexchange interaction of Fe^{3+} ions [5,14, 16–18]. As the Sr content increases, the Néel temperature decreases [14, 15]. For samples within the $0 \leq x \leq 0.3$ composition range, a weak

* Corresponding author. Lomonosov Moscow State University, GSP-1, Leninskie Gory, Moscow, 119991, Russia.
** Corresponding author. Institute of Solid State Physics, Russian Academy of Sciences, Academician Ossipyan 2, Chernogolovka, Moscow District, 142432, Russia.
E-mail addresses: sedykh@issp.ac.ru (V. Sedykh), di.pchelina@physics.msu.ru (D. Pchelina).

https://doi.org/10.1016/j.jpcs.2022.111001
Received 31 January 2022; Received in revised form 6 September 2022; Accepted 7 September 2022
Available online 16 September 2022

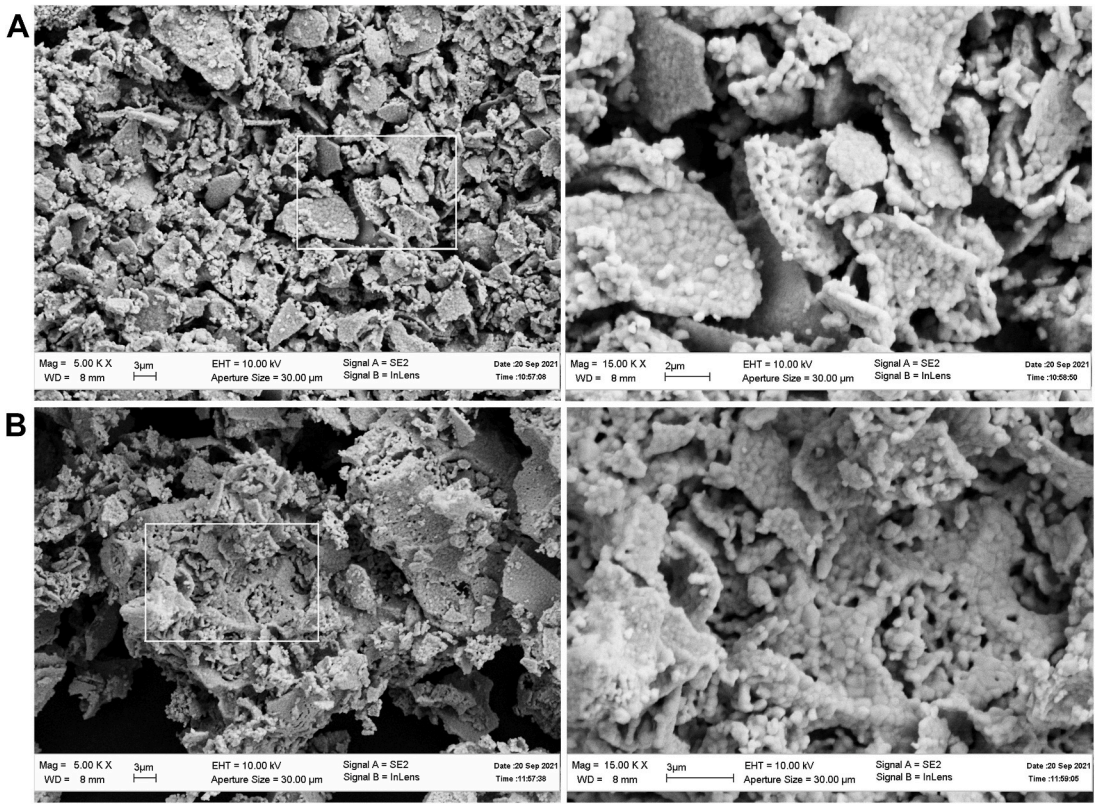

Fig. 1. SEM images: (a, a1) as-synthesized $La_{0.67}Sr_{0.33}FeO_{3-\gamma}$ sample and (b, b1) sample annealed in vacuum at 650 °C.

ferromagnetism with spontaneous magnetization was observed, which decreased with an increase in Sr amount in the ferrite [19]. Weak ferromagnetism is associated with a slight canting of Fe ions' magnetic moments as a result of an oxygen octahedral arrangement in a zigzag manner.

Annealing of $La_{1-x}Sr_xFeO_{3-\gamma}$ oxide in a vacuum leads to the formation of oxygen vacancies and, correspondingly, to the unit cell volume increase. However, the Fe–Fe and Fe–O distances do not practically change. Only the change of mutual coordination of the oxygen octahedra occurs, increasing the Fe^{3+}–O^{2-}–Fe^{3+} linkage angle and, thus, the superexchange interaction among Fe^{3+} ions [3]. The latter effect and a change of Fe ion valence states govern the Néel temperature and magnetic properties of these materials. Variation of the heat treatment conditions leads to phase transformations in the compounds and changing in the electronic states of Fe ions.

The electronic state of Fe ions in the substituted lanthanum ferrites, as well as the changes in their nearest oxygen environment might be effectively explored using Mössbauer spectroscopy. In these oxides, the Mössbauer spectra of Fe ions with different states are a set of partial magnetic spectra with different Mössbauer parameters (effective magnetic fields, isomer, and quadrupole shifts). Consequently, complete or partial substitution of an alkaline earth element for La leads to a decrease in the effective magnetic field. The appearance of oxygen vacancies decreases the isomeric shift and increases the quadrupole shift [20,21]. The $La_{1-x}Sr_xFeO_{3-\gamma}$ polycrystalline samples in the Sr concentration range $0 \leq x \leq 0.4$ can be used to obtain a wide range of particle sizes (80–2000 nm) [5].

For most perovskites, breaking of ideal cubic symmetry results in appearance of the Raman-active optical phonons (LO) [22]. The strong connection of the electronic system with phonon lattice vibrations in perovskites leads to the extreme sensitivity of LO phonons to the oxygen content and the temperature dependence of their energy [22]. Pure lanthanum ferrite ($LaFeO_3$) has been actively studied for more than 30 years. However, only two papers on ferrites with the substitution of La^{3+} by Sr^{2+} or Ca^{2+} have been published so far [23,24]. For $La_{0.33}Sr_{0.67}FeO_3$ and $CaFeO_3$, distinct changes of LO phonon energies occurred below charge ordering temperature of Fe ions, as demonstrated by Raman spectroscopy [23]. The loss of oxygen upon annealing caused a transformation from a rhombohedral to a Brownmillerite-type structure in a thin $La_{0.2}Sr_{0.8}FeO_3$ film [24]. The transformation was accompanied by an increase in sample electrical resistivity and enhancement of the Raman peaks in the frequency range of 400–800 cm^{-1} due to the symmetry decrease [24].

In the present work, the nature of the structural changes in the substituted orthoferrite $La_{0.67}Sr_{0.33}FeO_{3-\gamma}$, valence states of the Fe atoms, and transitions to a magnetically ordered state caused by gradual removal of oxygen and the formation of oxygen vacancies were studied using scanning electron microscopy (SEM), X-ray diffraction (XRD), and Mössbauer and Raman spectroscopy.

2. Materials and methods

A polycrystalline sample $La_{0.67}Sr_{0.33}FeO_{3-\gamma}$ was prepared in air by a sol-gel method using strontium, iron, and lanthanum nitrates in a stoichiometric ratio and glycine as starting reagents. The details of the preparation procedure were previously described [25]. After synthesis at 1100 °C for 20 h in air, samples were cooled slowly in a furnace to room temperature. Then samples were annealed under vacuum (10^{-3} Torr) at 200–650°C for 4 h and cooled slowly.

The diffraction patterns of the as-synthesized and vacuum-annealed polycrystalline samples were monitored at room temperature on a Siemens-D500 diffractometer using CoKα radiation. For phase analysis, calculation of XRD patterns, and refinement of unit cell parameters, the Powder Cell 2.4 and Match 3 packages were used.

A Carl Zeiss Supra 50VP high-resolution scanning electron microscope equipped with INCA Energy + microanalysis system was used to monitor SEM images in secondary electrons applying accelerating voltage of 10 kV and at magnifications of 5000 × and 15000 × .

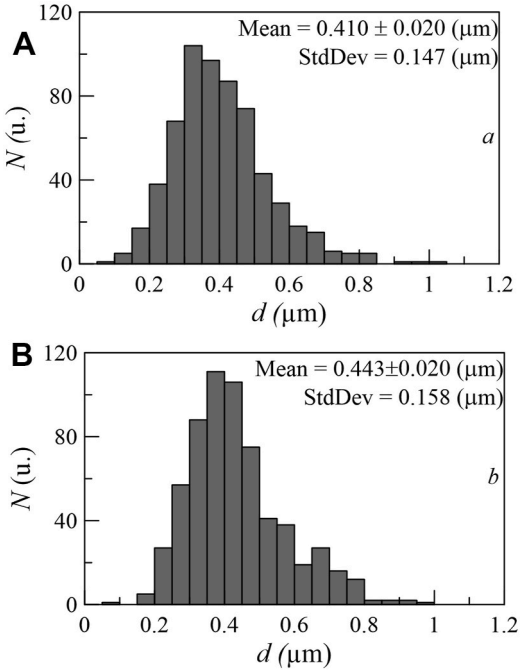

Fig. 2. Histograms of samples: (a) as-synthesized and (b) annealed in vacuum at 650°C.

Mössbauer measurements were performed at room temperature on polycrystalline samples on a CM 1101 spectrometer operating in a constant acceleration mode. Radioactive source was ^{57}Co (Rh). The fitting and analysis of the spectra were carried out using the distribution of hyperfine spectral parameters in the SpectrRelax program [26].

Raman spectra were measured at room temperature on a micro-Raman system operating in a backscattering geometry equipped with HRS-500 spectrometer. A diode KLM–532/SLN–100 laser with a wavelength of 532 nm was used for excitation; laser power on the sample was ~3 mW and diameter of the laser spot on the sample was ~5 μm. A razor edge filter and a Notch filter were used to discriminate the laser line. The spectral width of the setup was 200 cm^{-1}. Spectral resolution in the investigated frequency range was better than ~1 cm^{-1} with an experimental error of ±1 cm^{-1}.

3. Results and discussion

3.1. SEM results

The SEM images of the $La_{0.67}Sr_{0.33}FeO_{3-\gamma}$ sample microstructures are shown in Fig. 1. The analysis demonstrates that the samples are agglomerates of sintered particles. Particle size distribution histograms for as-synthesized samples and samples annealed under vacuum at 650 °C show that particle size depends slightly on vacuum annealing and average size is 0.41–0.44 μm (Fig. 2).

3.2. XRD analysis

The $LaFeO_3$ has an orthorhombic structure with the space group *Pbnm* (JCPDS 82–1958) and lattice parameters $a = 5.553$ Å, $b = 5.566$ Å, and $c = 7.851$ Å. The diffraction patterns of all $La_{0.67}Sr_{0.33}FeO_{3-\gamma}$ samples are similar, indicating absence of significant structural changes upon vacuum annealing. The diffraction patterns have a common feature of the diffraction lines broadening noticeably, especially at high diffraction angles. The broadening can be associated with the inhomogeneous distribution of Sr atoms at the La positions over the sample, and with spatial variations of the oxygen content, and, as a consequence, the inhomogeneity of the structure. The XRD pattern of the as-synthesized

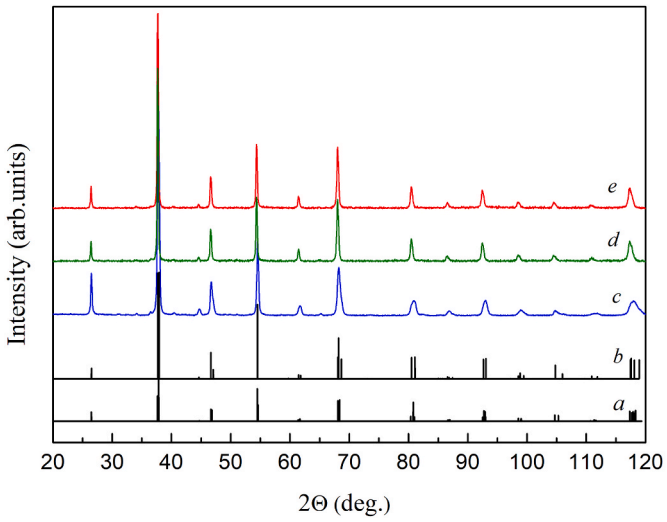

Fig. 3. Calculated diffraction patterns: (a) *Pbnm* and (b) *R-3c*. Diffraction patterns of $La_{0.67}Sr_{0.33}FeO_{3-\gamma}$ samples: (c) as-synthesized and annealed in vacuum at (d) 450 °C and (e) 650 °C.

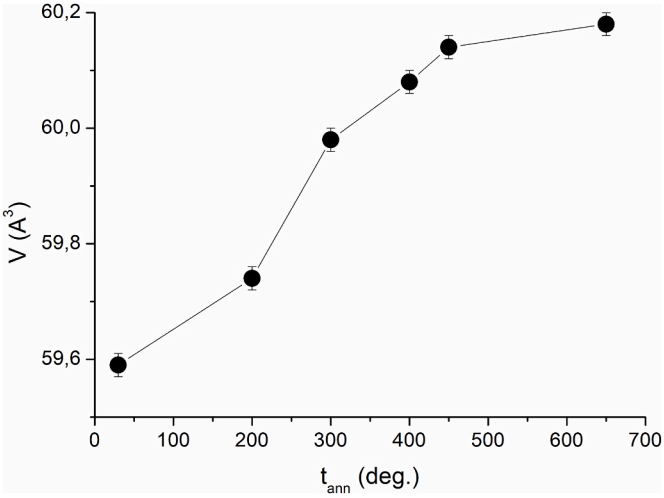

Fig. 4. Dependence of the pseudocubic cell volume V_{cell} $La_{0.67}Sr_{0.33}FeO_{3-\gamma}$ on the vacuum annealing temperature.

sample (Fig. 3) can be described by the known $La_{0.67}Sr_{0.33}FeO_3$ orthorhombic cell with space group *Pbnm* (JCPDS 89–1269) and lattice parameters $a = 5.502$ Å, $b = 5.544$ Å, and $c = 7.811$ Å. However, its interpretation in the assumption of a two-phase mixture, which additionally includes a certain proportion of the rhombohedral phase *R-3c* (JCPDS 49–0285), gives the best result. This fact is in accordance with previous results [17,27]. The structures of samples annealed under vacuum at temperatures of 200–400 °C are the same, and only the lattice parameters of the phases and the cell volumes change. The diffraction patterns of the samples annealed at 450 °C and 650 °C do not practically differ from each other, suggesting that the main structural changes finish at 450 °C. In this case, the last sample from the series has an orthorhombic lattice with $a = 5.535$ Å, $b = 5.548$ Å, and $c = 7.838$ Å, practically without an impurity of the rhombohedral phase.

The structure of both phases (*Pbnm* and *R–3c*) present in the sample is a perovskite lattice with slight distortions; therefore, the diffraction lines from them overlap to a large extent, which does not allow reliably establishing their quantitative ratio. In this case, it is convenient to use the pseudocubic perovskite cell volume to describe the ongoing changes. Volume of the pseudocubic cell V_{cell} is plotted as a function of the

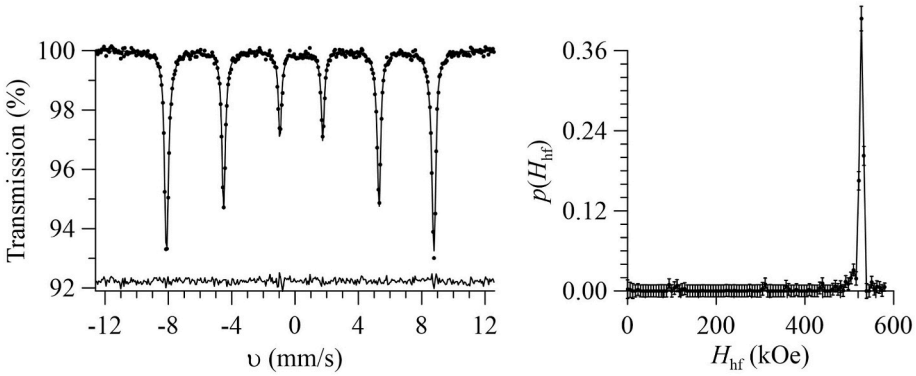

Fig. 5. Room-temperature Mössbauer spectrum of $LaFeO_3$ and the recovered distribution $p(H_{hf})$ of the hyperfine magnetic field H_{hf}.

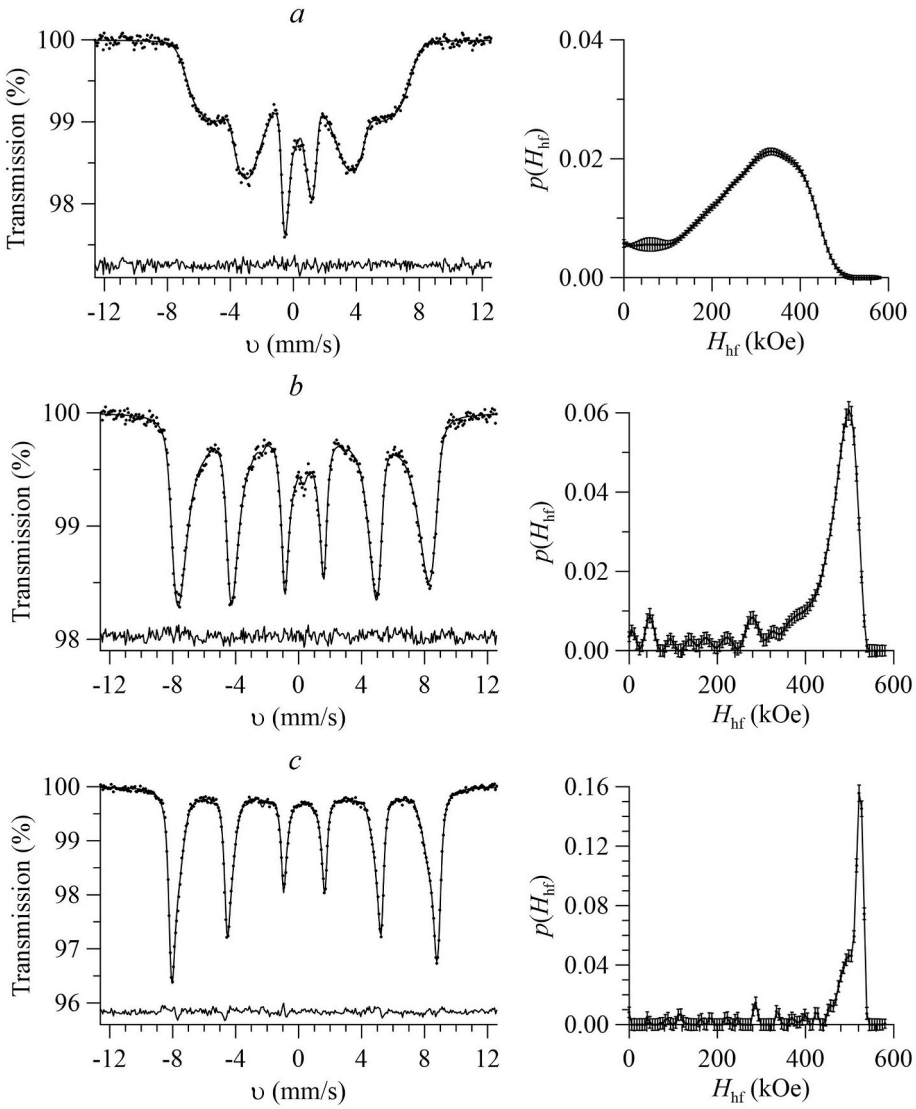

Fig. 6. Results of the recovering of hyperfine magnetic field H_{hf} for the Mössbauer spectra of $La_{0.67}Sr_{0.33}FeO_{3-\gamma}$ samples: (a) as-synthesized and annealed in vacuum (b) at 300°C and (c) 650°C.

vacuum annealing temperature (Fig. 4). A continuous increase of V_{cell} with annealing temperature is due to the reduction of oxygen content in the lattice (or increasing the number of oxygen vacancies). The V_{cell} levels out above 450 °C, indicating that the equilibrium state is attained at these temperatures (Fig. 4).

3.3. Mössbauer spectroscopy data

Fitting of the room-temperature Mössbauer spectra of $La_{0.67}Sr_{0.33}FeO_{3-\gamma}$ using application of several partial spectra is not applicable because of uncertainty both in the number of partial spectra

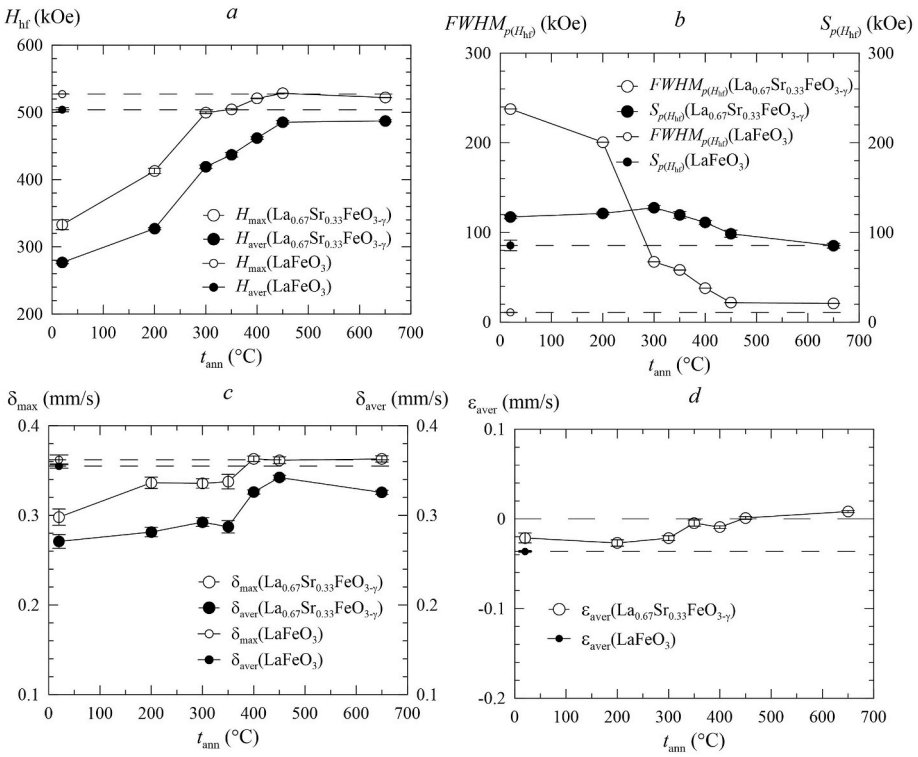

Fig. 7. Changes in the hyperfine parameters of the $La_{0.67}Sr_{0.33}FeO_{3-\gamma}$ Mössbauer spectrum with vacuum annealing temperature: average values (aver), values at the distribution maximum (max), half-height widths (*FWHM*), and standard deviations of the distribution for the (a, b) hyperfine magnetic field H_{hf}, (c) isomer shift δ and (d) quadrupole shift ε in comparison with data for unsubstituted lanthanum ferrite $LaFeO_3$.

and in the values of their hyperfine parameters. Therefore the method of recovering the distribution of spectrum parameters by the SpectrRelax program is used to fit the spectra [26]. The hyperfine magnetic field (H_{hf}) distribution [$p(H_{hf})$] is recovered for each Mössbauer spectrum taking into account its linear correlation with the isomeric shift (δ) at the desired average value of the quadrupole shift (ε) of its components.

The Mössbauer spectrum of pure $LaFeO_3$ is a typical Zeeman sextet associated with the magnetic ordering of lanthanum ferrite at room temperature (Fig. 5). The hyperfine parameters of the spectrum are in good agreement with known data [28] and correspond to Fe atoms in a trivalent high-spin state in an octahedral oxygen environment.

Substitution of La^{3+} by Sr^{2+} leads to a significant change of the Mössbauer spectrum compared to unsubstituted lanthanum ferrite (Fig. 6). The splitting of the spectrum is reduced noticeably, and the resonance lines are significantly broadened, corresponding to the appearance of a wide hyperfine magnetic field distribution. The Mössbauer spectra of some of the $La_{0.67}Sr_{0.33}FeO_{3-\gamma}$ samples after vacuum annealing are shown in Fig. 6. The annealing after synthesis leads to an increase in the magnetic splitting, and a narrowing and better resolving of the resonance lines in the spectrum.

The variations of hyperfine parameters of the Mössbauer spectra of $La_{0.67}Sr_{0.33}FeO_{3-\gamma}$ samples with the temperature of vacuum annealing are shown in Fig. 7 – average values (H_{aver}, δ_{aver}, and ε_{aver}), values at the distribution maximum (H_{max} and δ_{max}), width at half maximum $FWHM_{p(Hhf)}$, and the standard deviation $S_{p(Hhf)}$ of the distribution – compared to the data for unsubstituted $LaFeO_3$.

The difference between the hyperfine parameters of the as-synthesized and annealed $La_{0.67}Sr_{0.33}FeO_{3-\gamma}$ samples compared to those of $LaFeO_3$ are directly related to the possible appearance of Fe ions with increased valence and of oxygen vacancies upon the substitution of Sr^{2+} for La^{3+} and a change in their quantities upon further vacuum annealing.

It should be noted that there are several factors that significantly change in the spectra compared to lanthanum ferrite. For the as-synthesized sample, there is, first, a strong decrease in both H_{max} and H_{aver} when 33% La is replaced by Sr (Fig. 7*a*); second, a very wide $p(H_{hf})$ (Fig. 7*b*); and, third, a decrease in the isomer shift (Fig. 7*c*). The isomer shift value indicates that the Fe ions are in the averaged-valence state, i. e. with a fractional degree of oxidation. This may be due to the rapid (with a characteristic time $<10^{-8}$ s) transfer of electrons between the Fe ions at room temperature [29,30]. The spectrum resembles that of $La_{0.67}Sr_{0.33}FeO_{3-\gamma}$ [20]. According to the literature, Fe^{4+} ions do not manifest themselves in this range of Sr concentrations in Mössbauer measurements at room temperature. The very wide $p(H_{hf})$ can be due to two main factors. First, it is the random distribution of Sr^{2+} ions over the La^{3+} ion positions, in turn accompanied by a random distribution of Fe^{4+} ions over the Fe atom positions and by the appearance of randomly distributed oxygen vacancies in the structure of substituted ferrite $La_{0.67}Sr_{0.33}FeO_{3-\gamma}$. This distribution of ions and vacancies in the structure leads to a strong local inhomogeneity in the environment of Mössbauer Fe atoms. The second factor affecting the width of $p(H_{hf})$ is the fast transfer of electrons between Fe^{3+} and Fe^{4+} ions, which leads to the averaged-valence state of Fe atoms.

Attention is drawn to the fact that the average value of H_{aver} is noticeably less than the H_{max} value at the maximum of $p(H_{hf})$ (Fig. 7*a*). Let us consider the reasons for this. The $LaFeO_3$ contains only Fe^{3+} and has no oxygen vacancies. When 33% La atoms are replaced by Sr in $LaFeO_3$, Fe^{4+} ions appear in addition to Fe^{3+}. In the as-synthesized $La_{0.67}Sr_{0.33}FeO_{3-\gamma}$, the H_{max} is significantly lower than in $LaFeO_3$ due to the appearance of a significant amount of Fe^{4+} cations. As mentioned above, when Sr randomly substitutes La, a strong local inhomogeneity in the environment of Mössbauer Fe atoms appears, resulting in a difference in the H_{max} and H_{aver} field values. We assume that the as-synthesized sample contains a sufficiently large amount of Fe^{4+} and a minimum amount of oxygen vacancies.

The values of H_{aver} and δ_{aver}, as well as of H_{max} and δ_{max}, increase with an increase of vacuum annealing temperature t_{ann}, and, thus, with an increase in amount of oxygen vacancies (Fig. 7*b*). The width at half

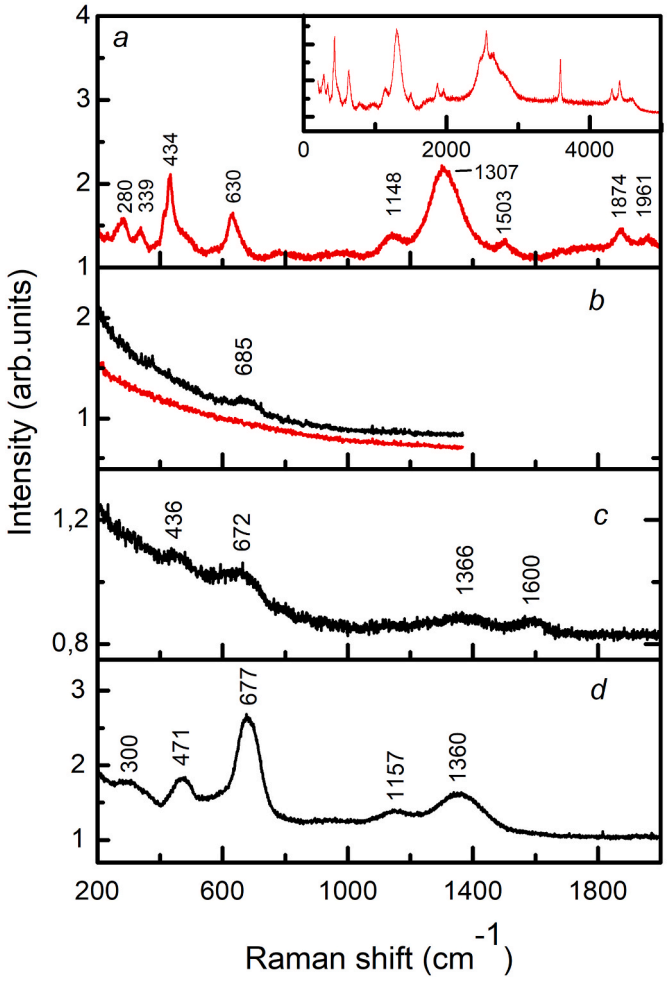

Fig. 8. (a) Raman spectra of as-synthesized $LaFeO_3$ sample. The inset shows the spectrum of the same sample in a wide frequency range. Room-temperature Raman spectra of $La_{1-x}Sr_xFeO_{3-\gamma}$ samples: (b) as-synthesized sample, black and red curves – spectra of two different points on the sample – and samples annealed in vacuum at (c) 300 °C and (d) 650 °C. Numbers indicate the position of the peak maxima in cm^{-1}.

maximum $FWHM_{p(Hhf)}$ and the standard deviation $S_{p(Hhf)}$ of the $p(H_{hf})$ decrease with t_{ann}. This indicates a decrease of the amount of Fe^{4+} ions in the annealed sample. At $t_{ann} \geq 450$ °C, there are practically no Fe^{4+} ions and an averaged-valence state of Fe atoms, when the δ_{aver} and δ_{max} values reach the Fe^{3+} characteristic values, and oxygen stops leaving the ferrite lattice. In the range of annealing temperatures of 450–650 °C, the H_{aver} and δ_{aver} values, as well as of H_{max} and δ_{max}, reach their maximum, and $FWHM_{p(Hhf)}$ and $S_{p(Hhf)}$ of $p(H_{hf})$ reach their minimum values, which practically coincide with similar values for $LaFeO_3$. The average value of the quadrupole shift ε in the spectrum of the as-synthesized sample turns out to be negative and somewhat lower in absolute value than that for $LaFeO_3$ (Fig. 7d).

3.4. Raman spectroscopy

The assignment of phonon modes of lanthanum orthoferrites in the frequency range below 1000 cm^{-1} was previously considered [22,31]. Modes below 200 cm^{-1} in $LaFeO_3$ refer to lattice vibrations of heavy La atoms, modes between 200 and 450 cm^{-1} refer to oxygen vibrations in the tilted FeO_6 octahedra, and modes at ~630 cm^{-1} indicate in-phase stretching of Fe–O bonds [22]. The modes above 1000 cm^{-1} in $LaFeO_3$ are usually referred to as two-magnon scattering [6]. However, this interpretation of the Raman active modes for lanthanum ferrites is not definitive [22].

The room-temperature Raman spectra of $LaFeO_3$ and $La_{0.67}Sr_{0.33}FeO_{3-\gamma}$ samples, as-synthesized and after vacuum annealing at 300 °C and 650 °C, show the correspondence for Raman peaks for the $La_{0.67}Sr_{0.33}FeO_{3-\gamma}$ samples annealed in vacuum with the main Raman peaks for the $LaFeO_3$ at ~280, ~339, ~434, and ~630 cm^{-1} (Fig. 8). Annealing of $La_{0.67}Sr_{0.33}FeO_{3-\gamma}$ leads to smearing and even merging of adjacent Raman lines characteristic of $LaFeO_3$ into one broad fringe. For example, the ~280 and ~339 cm^{-1} lines for $LaFeO_3$ (Fig. 8a) are transformed into single rather broad fringe at ~300 cm^{-1} for the $La_{0.67}Sr_{0.33}FeO_{3-\gamma}$ sample annealed in vacuum at 650°C (Fig. 8d). Similarly, the ~434 and ~630 cm^{-1} lines for $LaFeO_3$ are transformed to the extended fringes at ~436 and ~672 cm^{-1}, respectively, for the $La_{0.67}Sr_{0.33}FeO_{3-\gamma}$ sample annealed at 300°C (Fig. 8c). These fringes shift to even higher frequencies, to ~471 and ~677 cm^{-1} positions, respectively, for the $La_{0.67}Sr_{0.33}FeO_{3-\gamma}$ sample annealed at 650°C (Fig. 8d).

It is worth noting that 436–470 and ~670 cm^{-1} lines appearing after vacuum annealing are most intensive and clearly expressed only in the sample annealed at 650 °C when there is already no averaged-valence state of Fe atoms, and all Fe atoms are in Fe^{3+} state, and oxygen stops leaving the lattice under annealing. At the same time, in the as-synthesized sample, in which there is a sufficiently large number of Fe^{4+} ions and, apparently, the minimum number of oxygen vacancies, even weak and broad lines of phonon mode vibrations at ~685 cm^{-1} are recognized for the few sample particles only, and their fraction is less than 10% (compare black and red curves in Fig. 8b). Only vacuum annealing at 200 °C and above gives a very weak but well-reproducible Raman spectra of each individual particle of polycrystalline samples as, for example, the spectrum of the sample annealed at 300 °C (Fig. 8c). It is natural to associate a significant broadening of all Raman lines in $La_{0.67}Sr_{0.33}FeO_{3-\gamma}$ with the local disorder arising when La is substituted by Sr. This effect leads to a strong inhomogeneity of the Fe^{4+}/Fe^{3+} ion charge state and associated oxygen vacancies in their nearest environment appearing under vacuum annealing.

Only studies in a wide temperature range below and above the Néel temperature ($T_N = 740$ K [7,13]) similar to a previous report [6] might give an unambiguous Raman mode assignment.

4. Conclusion

All the samples were agglomerates of sintered particles, with size depending slightly on annealing in vacuum, and average size was 0.41–0.44 μm.

Upon vacuum annealing, no significant structural changes were observed. The volume of the pseudocubic cell V_{cell} increased continuously with vacuum annealing temperature, and the main structural changes finished at temperatures above 450 °C.

The Fe^{4+} ions in $La_{0.67}Sr_{0.33}FeO_{3-\gamma}$ did not appear at room temperature as a particular Mössbauer subspectrum. Their presence resulted in a wide distribution of the hyperfine magnetic field corresponding to the averaged-valence state of Fe atoms, which was due to the rapid transfer of electrons between Fe^{3+} and Fe^{4+} ions in a locally inhomogeneous ionic environment. The appearance of this state was associated with the substitution of 33% La by Sr in $LaFeO_3$. Vacuum annealing led to an increase of the hyperfine magnetic field on ^{57}Fe nuclei and an isomer shift of the Mössbauer spectrum with an increase of annealing temperature, which was caused by an increase in the number of vacancies and, respectively, a decrease in the amount of Fe^{4+}. The averaged-valence state of Fe atoms almost disappeared at temperatures of 450°C and higher, with Fe^{3+} ions only present and the amount of oxygen vacancies stabilized; the Mössbauer parameters stopped changing in the temperature range of 450–650 °C, and the process of oxygen leaving the crystal lattice under vacuum annealing ceased.

For as-synthesized $La_{0.67}Sr_{0.33}FeO_{3-\gamma}$ the Raman spectra revealed that substitution of 33% La by Sr atoms led to the presence of the lone

broad fringe at ~685 cm^{-1} as compared to $LaFeO_3$. With increasing vacuum annealing temperature, new fringes appeared in Raman spectra. Thus, the band frequencies for the sample annealed at 650 °C corresponded to the peak positions of the unsubstituted $LaFeO_3$. Evolution of the $La_{0.67}Sr_{0.33}FeO_{3-\gamma}$ Raman spectra observed with annealing temperature correlated with the changes of the Fe atoms' valence state revealed by Mössbauer spectroscopy. The observed significant broadening of peaks, compared to $LaFeO_3$, was associated with the random distribution of Sr^{2+} ions over the La^{3+} positions and, hence, with a random distribution of Fe^{4+} atoms over the Fe atom positions in the structure of the substituted $La_{0.67}Sr_{0.33}FeO_{3-\gamma}$ ferrite.

Analysis of the results for $La_{0.67}Sr_{0.33}FeO_{3-\gamma}$ demonstrated good correlations among the XRD, Mössbauer, and Raman spectroscopy data. A detailed study of as-synthesized and annealed ferrite samples at low temperatures is required in order to elucidate the changes of Fe ions' valence state as well as of their environment. The results of these studies will be published later.

Author statement

V. Sedykh: Supervision, Conceptualization, Investigation, Writing - Original Draft, **O. Rybchenko**: Investigation, Formal analysis, **V. Rusakov:** Conceptualization, Writing - Original Draft, **S. Zaitsev**: Investigation, Writing - Review & Editing, **O. Barkalov**: Investigation, Writing - Review & Editing, **E. Postnova**: Investigation, **T. Gubaidulina**: Visualization, **D. Pchelina**: Visualization, Formal analysis, **V. Kulakov**: Formal analysis.

Declaration of competing interest

The authors declare that they have no known competing financial interests or personal relationships that could have appeared to influence the work reported in this paper.

Data availability

No data was used for the research described in the article.

Acknowledgments

Raman measurements were carried out on a spectrometer of the Center for Collective Using in the Institute of Solid State Physics, Russian Academy of Sciences. Diana Pchelina is a scholarship holder of the Foundation for the Development of Theoretical Physics and Mathematics "BASIS" No21-2-2-37-1.

References

[1] M.B. Salamon, M. Jaime, The physics of manganites: structure and transport, Rev. Mod. Phys. 73 (2001) 583–628, https://doi.org/10.1103/REVMODPHYS.73.583.
[2] Y. Tokura (Ed.), Contribution to Colossal Magnetoresistance Oxides, Gordon & Breach, London, 1999.
[3] J.B. Yang, W.B. Yelon, W.J. James, Z. Chu, M. Kornecki, Y.X. Xie, X.D. Zhou, H. U. Anderson, A.G. Joshi, S.K. Malik, Crystal structure, magnetic properties, and Mössbauer studies of $La_{0.6}Sr_{0.4}FeO_{3-d}$ prepared by quenching in different atmospheres, Phys. Rev. B 66 (2002), 184415, https://doi.org/10.1103/PhysRevB.66.184415.
[4] J.B. Goodenough, Metallic oxides, Prog. Solid State Chem. 5 (1971) 145–399.
[5] R.B. da Silva, J.M. Soares, J.A.P. da Costa, J.H. de Araújo, A.R. Rodrigues, F.L. A. Machado, Local iron ion distribution and magnetic properties of the perovskites $La_{1-x}Sr_xFeO_{3-\gamma}$, J. Magn. Magn Mater. 466 (2018) 306–310, https://doi.org/10.1016/J.JMMM.2018.07.040.
[6] S. Manzoor, S. Husain, Analysis of Zn substitution on structure, optical absorption, magnetization, and high temperature specific heat anomaly of the nano-crystalline $LaFeO_3$, J. Appl. Phys. 124 (2018), 065110, https://doi.org/10.1063/1.5025252.
[7] S. Phokha, S. Pinitsoontorn, S. Rujirawat, S. Maensiri, Polymer pyrolysis synthesis and magnetic properties of $LaFeO_3$ nanoparticles, Phys. B Condens. Matter 476 (2015) 55–60, https://doi.org/10.1016/J.PHYSB.2015.07.021.
[8] E.A. Tugova, V.F. Popova, I.A. Zvereva, V.V. Gusarov, Phase diagram of the $LaFeO_3$-$LaSrFeO_4$ system, Glas, Phys. Chem. 32 (2006) 674–676, https://doi.org/10.1134/S1087659606060137.
[9] S. Petrović, A. Terlecki-Baričević, L. Karanović, P. Kirilov-Stefanov, M. Zdujić, V. Dondur, D. Paneva, I. Mitov, V. Rakić, $LaMO_3$ (M = Mg, Ti, Fe) perovskite type oxides: preparation, characterization and catalytic properties in methane deep oxidation, Appl. Catal. B Environ. 79 (2008) 186–198, https://doi.org/10.1016/J.APCATB.2007.10.022.
[10] S.N. Tijare, M.V. Joshi, P.S. Padole, P.A. Mangrulkar, S.S. Rayalu, N.K. Labhsetwar, Photocatalytic hydrogen generation through water splitting on nano-crystalline $LaFeO_3$ perovskite, Int. J. Hydrogen Energy 37 (2012) 10451–10456, https://doi.org/10.1016/J.IJHYDENE.2012.01.120.
[11] Z.X. Wei, Y.Q. Xu, H.Y. Liu, C.W. Hu, Preparation and catalytic activities of $LaFeO_3$ and Fe_2O_3 for HMX thermal decomposition, J. Hazard Mater. 165 (2009) 1056–1061, https://doi.org/10.1016/J.JHAZMAT.2008.10.086.
[12] J. Faye, A. Baylet, M. Trentesaux, S. Royer, F. Dumeignil, D. Duprez, S. Valange, J. M. Tatibouët, Influence of lanthanum stoichiometry in $La_{1-x}FeO_{3-\delta}$ perovskites on their structure and catalytic performance in CH_4 total oxidation, Appl. Catal. B Environ. 126 (2012) 134–143, https://doi.org/10.1016/J.APCATB.2012.07.001.
[13] J.B. Goodenough, in: F. Albert Cotton (Ed.), Magnetism and Chemical Bond, vol. 1, Interscience, London, 1963.
[14] U. Shimony, J.M. Knudsen, Mössbauer studies on iron in the perovskites $La_{1-x}Sr_xFeO_3$ (0<~x<~1), Phys. Rev. 144 (1966) 361, https://doi.org/10.1103/PhysRev.144.361.
[15] J.C. Grenier, N. Ea, M. Pouchard, M. Abou-Sekkina, Proprietes electriques et magnetiques des ferrites oxydes $La_{1-x}Sr_xFeO_{3-y}$, Mater. Res. Bull. 19 (1984) 1301–1309, https://doi.org/10.1016/0025-5408(84)90192-2.
[16] M. Takano, J. Kawachi, N. Nakanishi, Y. Takeda, Valence state of the Fe ions in $Sr_{1-y}La_yFeO_3$, J. Solid State Chem. 39 (1981) 75–84, https://doi.org/10.1016/0022-4596(81)90304-2.
[17] S.E. Dann, D.B. Currie, M.T. Weller, M.F. Thomas, A.D. Al-Rawwas, The effect of oxygen stoichiometry on phase relations and structure in the system $La_{1-x}Sr_xFeO_{3-\delta}$ ($0 \le x \le 1$, $0 \le \delta \le 0.5$), J. Solid State Chem. 109 (1994) 134–144, https://doi.org/10.1006/JSSC.1994.1083.
[18] A.D. Al-Rawwas, C.E. Johnson, M.F. Thomas, S.E. Dann, M.T. Weiler, Mössbauer studies on the series $La_{1-x}Sr_xFeO_3$, Hyperfine Interact. 93 (1994) 1521–1529, https://doi.org/10.1007/BF02072903.
[19] J. Li, X. Kou, Y. Qin, H. He, Microstructure and magnetic properties of La1—xSrxFeO3 nanoparticles, Phys. Status Solidi A 191 (2002) 255–259, https://doi.org/10.1002/1521-396X(200205)191:1%3C255::AID-PSSA255%3E3.0.CO;2-N.
[20] G. Li, L. Li, M. Zhao, The study of ^{57}Fe Mössbauer spectra for $La_{0.7}Sr_{0.3}FeO_{3-\delta}$ with different structure, Phys. Status Solidi B 197 (1996) 165–172, https://doi.org/10.1002/PSSB.2221970123.
[21] H. Yamamura, R. Kiriyama, Oxygen vacancies in the perovskite-type ferrites. II. Mössbauer effect in the $SrFeO_{2.5}$-$LaFeO_3$ solid-solution system, Bull. Chem. Soc. Jpn. 45 (2006) 2702–2708, https://doi.org/10.1246/BCSJ.45.2702.
[22] J. Andreasson, J. Holmlund, C.S. Knee, M. Käll, L. Börjesson, S. Naler, J. Bäckström, M. Rübhausen, A.K. Azad, S.G. Eriksson, Franck-Condon higher order lattice excitations in the $LaFe_{1-x}Cr_xO_3$ (x=0, 0.1, 0.5, 0.9, 1.0) perovskites due to Fe-Cr charge transfer effects, Phys. Rev. B Condens. Matter 75 (2007), 104302, https://doi.org/10.1103/PHYSREVB.75.104302.
[23] S. Ghosh, N. Kamaraju, M. Seto, A. Fujimori, Y. Takeda, S. Ishiwata, S. Kawasaki, M. Azuma, M. Takano, A.K. Sood, Raman scattering in $CaFeO_3$ and $La_{0.33}Sr_{0.67}FeO_3$ across the charge-disproportionation phase transition, Phys. Rev. B Condens. Matter 71 (2005), 245110, https://doi.org/10.1103/PHYSREVB.71.245110.
[24] M.A. Islam, Y. Xie, M.D. Scafetta, S.J. May, J.E. Spanier, Raman scattering in $La_{1-x}Sr_xFeO_{3-\delta}$ thin films: annealing-induced reduction and phase transformation, J. Phys. Condens. Matter 27 (2015), 155401, https://doi.org/10.1088/0953-8984/27/15/155401.
[25] V.D. Sedykh, O.G. Rybchenko, A.N. Nekrasov, I.E. Koneva, V.I. Kulakov, Effect of the oxygen content on the local environment of Fe atoms in anion-deficient $SrFeO_{3-\delta}$, Phys. Solid State 61 (2019) 1099–1106, https://doi.org/10.1134/S1063783419060210.
[26] M.E. Matsnev, V.S. Rusakov, SpectrRelax: an application for Mössbauer spectra modeling and fitting, in: AIP Conf. Proc., American Institute of Physics, 2012, pp. 178–185, https://doi.org/10.1063/1.4759488.
[27] A. Fossdal, M. Menon, I. Wærnhus, K. Wiik, M.A. Einarsrud, T. Grande, Crystal structure and thermal expansion of $La_{1-x}Sr_xFeO_{3-\delta}$ materials, J. Am. Ceram. Soc. 87 (2004) 1952–1958, https://doi.org/10.1111/J.1151-2916.2004.TB06346.X.
[28] J.C. Grenier, L. Fournès, M. Pouchard, P. Hagenmuller, S. Komornicki, Mössbauer resonance studies on the $Ca_2Fe_2O_5$-$LaFeO_3$ system, Mater. Res. Bull. 17 (1982) 55–61, https://doi.org/10.1016/0025-5408(82)90183-0.
[29] P.D. Battle, T.C. Gibb, S. Nixon, A study of the ordering of oxygen vacancies in the nonstoichiometric perovskite $Sr_2LaFe_3O_{8+y}$ by Mössbauer spectroscopy and a comparison with $SrFeO_{3-y}$, J. Solid State Chem. 79 (1989) 75–85, https://doi.org/10.1016/0022-4596(89)90252-1.
[30] P.D. Battle, T.C. Gibb, S. Nixon, A study of charge disproportionation in the nonstoichiometric perovskite $Sr_2LaFe_3O_{8+y}$ by Mössbauer spectroscopy, J. Solid State Chem. 77 (1988) 124–131, https://doi.org/10.1016/0022-4596(88)90099-0.
[31] M.N. Iliev, M.V. Abrashev, J. Laverdière, S. Jandl, M.M. Gospodinov, Y.Q. Wang, Y. Y. Sun, Distortion-dependent Raman spectra and mode mixing in $RMnO_3$ perovskites (R=La,Pr,Nd,Sm,Eu,Gd,Tb,Dy,Ho,Y), Phys. Rev. B Condens. Matter 73 (2006), 064302, https://doi.org/10.1103/PHYSREVB.73.064302/FIGURES/4/MEDIUM.